Top-quark forward-backward asymmetry in e^+e^- annihilation at NNLO in QCD

Jun Gao[1, 2, *] and Hua Xing Zhu[3, †]

[1] *Department of Physics, Southern Methodist University, Dallas, TX 75275-0175, USA*
[2] *High Energy Physics Division, Argonne National Laboratory, Argonne, IL 60439, USA*
[3] *SLAC National Accelerator Laboratory, Stanford University, Stanford, CA 94309, USA*

We report on a complete calculation of electroweak production of top quark pairs in e^+e^- annihilation at next-to-next-to-leading order in Quantum Chromodynamics. Our setup is fully differential and can be used to calculate any infrared-safe observable. Especially we calculated the next-to-next-to-leading order corrections to top-quark forward-backward asymmetry and found sizable effects. Our results show a large reduction of the theoretical uncertainties in predictions of the forward-backward asymmetry, and allow a precision determination of the top quark electroweak couplings at future e^+e^- colliders.

arXiv:1410.3165v1 [hep-ph] 12 Oct 2014

Introduction. Top-antitop quark pairs can be copiously produced at future International Linear Collider (ILC), facilitating a detailed study of top quark properties [1]. The clean enviorement of lepton collider allows measurement of the process $e^+e^- \to t\bar{t}$ to very high accuracy, which also demands high precision in theoretical calculation, in particular the inclusion of higher order QCD radiative corrections. In the past, significant theoretical efforts have been focused on $t\bar{t}$ production at threshold, for which Next-to-Next-to-Leading Order (NNLO) QCD corrections are known for more than a decade [2], and even next-to-next-to-next-to-leading order QCD corrections will be available in the near future [3]. However, for $t\bar{t}$ production in the continuum only total cross sections are known in high energy expansion [4]. Ingredients for a fully differential NNLO calculation in the continuum have been obtained by different groups [5, 6]. Recently, we reported a fully differential NNLO calculation for the photon mediated contributions [7], using a NNLO generalization of phase space slicing method [8, 9]. [1] In this Letter, we complete this calculation by including also the SM Z boson contributions.

As an important application of our results, we consider the calculation of top-quark forward-backward asymmetry (A_{FB}) at NNLO in e^+e^- collision in the continuum. In the limit of small top quark mass, this observable has been computed to NNLO in refs. [12]. The full mass effects are only known for the pure two-loop virtual contributions [13]. We report in this Letter the first calculation of full NNLO QCD corrections to this observable, including both loop contributions and real-radiation contributions. A_{FB} is an important precision observable for the determination of neutral-current electroweak couplings of top quark with photon and Z boson. Their precise measurement is an important probe of physics beyond Standard Model, *e.g.* Randall-Sundrum models [14], models of compositeness [15]. The information of top quark neutral coupling is encoded in the top-quark form factor. For on-shell $t\bar{t}$ pair, the form factor can be expressed by four independent scalar form factors,

$$\Gamma_\mu^{ttV}(Q_\mu) = -ie\left[\gamma_\mu\Big(F_{1v}^V(Q^2)+\gamma_5 F_{1a}^V(Q^2)\Big) + \left(\frac{\sigma_{\mu\nu}}{2m_t}Q^\nu\Big(iF_{2v}^V(Q^2)+\gamma_5 F_{2a}^V(Q^2)\Big)\right)\right] \quad (1)$$

where Q_μ is the total four-momentum of $t\bar{t}$, e is the positron charge, and m_t is the top-quark mass. V denotes photon (γ) or Z boson. To Leading Order (LO) in electroweak theory and QCD, the vector and axial form factors, $F_{1v}^V(Q^2)$ and $F_{1a}^V(Q^2)$, are given respectively by

$$F_{1v}^\gamma = Q_t\ , \quad F_{1a}^\gamma = 0\ ,$$
$$F_{1v}^Z = \frac{1}{\sin 2\vartheta}\left(\frac{1}{2}-2Q_t\sin^2\vartheta\right)\ , \quad F_{1a}^Z = \frac{-1}{2\sin 2\vartheta} \quad (2)$$

$Q_t = 2/3$ is the top-quark charge in unit of e, and ϑ is the weak-mixing angle. At ILC the top-quark forward-backward asymmetry can be measured to a precision of about one percent in relative, through both the full hadronic or semi-leptonic channels [16–18]. Correspondingly the above form factors will be determined much more precisely as compared to at the LHC [17], and thus provides strong sensitivity to any new physics that could modify the top-quark electroweak couplings. In this Letter, we computed the NNLO QCD corrections to the fully differential production of top quark pair, thereby obtain the A_{FB} at NNLO for the first time. Our calculation provides the most precise predictions on A_{FB} including its theoretical uncertainties, and also allows corrections for experimental acceptance using the full kinematic information.

The formalism. A fully differential calculation for $e^+e^- \to t\bar{t}$ at NNLO in QCD involves three types of diagrams, namely the two-loop virtual diagrams, one-loop real-virtual diagrams, and double real-emission diagrams. The individual contributions of these diagrams are known for some time, but combining them in a consistent way is a non-trivial task due to the presence of infrared singularities in QCD matrix elements. To this end, we employ

[1] Independently, calculation of inclusive cross section for $e^+e^- \to \gamma^* \to t\bar{t}$ at NNLO based on massive generalization of antenna subtraction method [10] has been reported recently in ref. [11].

a NNLO generalization phase-space slicing method, described in detail in a previous publication [7]. We briefly summarize its essential features here.

In perturbative QCD, differential cross section for any infrared-safe observable O has the schematic form

$$\frac{\mathrm{d}\sigma}{\mathrm{d}O} = \int \mathrm{d}PS_{t\bar{t}+X} |\mathcal{M}_{e^+e^-\to t\bar{t}X}|^2 \delta\Big(O - F(\{p_i\})\Big) \ , \quad (3)$$

where O is calculated from the set of final-state momentum $\{p_i\}$ through the measurement function F. Inserting a unit decomposition $1 = \Theta(\lambda - E_X) + \Theta(E_X - \lambda) \equiv \Theta_{\rm I} + \Theta_{\rm II}$, we can write Eq. (3) as

$$\frac{\mathrm{d}\sigma}{\mathrm{d}O} = \frac{\mathrm{d}\sigma_{\rm I}}{\mathrm{d}O} + \frac{\mathrm{d}\sigma_{\rm II}}{\mathrm{d}O} \ , \quad (4)$$

where

$$\frac{\mathrm{d}\sigma_{\rm I}}{\mathrm{d}O} = \int \mathrm{d}PS_{t\bar{t}+X} |\mathcal{M}_{e^+e^-\to t\bar{t}X}|^2 \delta\Big(O - F(\{p_i\})\Big)\Theta_{\rm I} \ ,$$
$$\frac{\mathrm{d}\sigma_{\rm II}}{\mathrm{d}O} = \int \mathrm{d}PS_{t\bar{t}+X} |\mathcal{M}_{e^+e^-\to t\bar{t}X}|^2 \delta\Big(O - F(\{p_i\})\Big)\Theta_{\rm II}$$

Obtaining $\mathcal{O}(\alpha_s^2)$ corrections to $\mathrm{d}\sigma/\mathrm{d}O$ simply amounts to achieving the same order of accuracy for $\mathrm{d}\sigma_{\rm I}/\mathrm{d}O$ and $\mathrm{d}\sigma_{\rm II}/\mathrm{d}O$. For $\mathrm{d}\sigma_{\rm II}/\mathrm{d}O$ this is simple. The presence of theta function $\Theta_{\rm II}$ implies that there is at least one parton other than the $t\bar{t}$ pair in the final state. This parton has the effect of regulating the so-called double-unresolved divergences in the QCD matrix elements. The only infrared divergences (soft or collinear) are of NLO origin and can be easily dealt with using any NLO subtraction scheme [19, 20]. In other words, the $\mathcal{O}(\alpha_s^2)$ contributions to $\mathrm{d}\sigma_{\rm II}/\mathrm{d}O$ can be obtained from a standard NLO QCD calculation for $e^+e^- \to t\bar{t}j$ [6]. The results will exhibit logarithmic singular dependence on the artificial parameter λ. Be specific, we employ the massive version of dipole subtraction method [20]. The one-loop real-virtual calculation is carried out by the automated program `GoSam2.0` [21] with loop integral reductions from `Ninja` [22, 23] and scalar integrals from `OneLOop` [24, 25]. Note that when $\sqrt{s} > 4m_t$, the channel for production of $t\bar{t}t\bar{t}$ is open. However, these additional contributions are themselves infrared finite and small for the energy range considered here, thus are not included. Similarly, we do not include the real emmision diagrams of which γ^*/Z^* couples to light or bottom quarks and the top quarks emitting from gluon splliting. Those contributions are also small, and espeially do not contribute to the top-quark FB asymmetry.

The calculation of $\mathrm{d}\sigma_{\rm I}/\mathrm{d}O$ is substantially more involved. However, significant simplification can be achieved if $\lambda \ll m_t$ [2]. In that regime, universal factorization properties of QCD matrix elements allow to write the distribution as *soft-virtual* contributions plus power suppressed terms

$$\frac{\mathrm{d}\sigma_{\rm I}}{\mathrm{d}O} = \frac{\mathrm{d}\sigma_{\rm s.v.}}{\mathrm{d}O} + \mathcal{O}\left(\frac{\lambda}{m_t}\right) \ , \quad (5)$$

where a soft expansion has been performed in $\mathrm{d}\sigma_{\rm s.v.}/\mathrm{d}O$ through the phase-space volume, the matrix elements, and the measurement function. As explained in ref. [7], the soft-virtual contributions have the form of factorized product of hard function and soft function, each of which is known to $\mathcal{O}(\alpha_s^2)$ in analytical form. The hard function is essentially the heavy quark form factors calculated in refs. [5], and the soft function is the phase-space integral in the eikonal limit. The soft function is the same for γ or Z meadiated contributions. Comparing with the vector contributions calculated in ref. [7], the only difference is the inclusion of axial-vector and anomaly contributions in the hard function. We note that $\mathrm{d}\sigma_{\rm s.v.}/\mathrm{d}O$ also exhibits logarithmic singular dependence on λ.

Combining $\mathrm{d}\sigma_{\rm s.v.}/\mathrm{d}O$ and $\mathrm{d}\sigma_{\rm II}/\mathrm{d}O$, we obtain a formally exact results for $\mathrm{d}\sigma/\mathrm{d}O$, in the limit $\lambda \to 0$. However, such a limit can never be reached because $\mathrm{d}\sigma_{\rm II}/\mathrm{d}O$ is usually computed numerically. In pratice, we choose the parameter sufficently small such that the power suppressed terms can be safely neglected, and the kinematical approximation in the soft-virtual contributions can be justified. The appropriate choice of λ can be indicated by searching for an region in which the dependence of λ in $\mathrm{d}\sigma_{\rm s.v.}/\mathrm{d}O + \mathrm{d}\sigma_{\rm II}/\mathrm{d}O$ is minimized.

Total cross sections. We first present our numeric results on total cross sections. We use two-loop running of the QCD coupling constants with $N_l = 5$ active quark flavors and $\alpha_s(M_Z) = 0.118$. We choose the G_F parametrization scheme [26] for the electroweak couplings with $M_W = 80.385\,\mathrm{GeV}$, $M_Z = 91.1876\,\mathrm{GeV}$, $M_t = 173\,\mathrm{GeV}$, and $G_F = 1.166379 \times 10^{-5}\,\mathrm{GeV}^{-2}$ [27]. The renormalization scale is set to the center of mass energy $\sqrt{s}$ unless otherwise specified. The production cross sections through to NNLO in QCD can be expressed as

$$\sigma_{NNLO} = \sigma_{LO}\left(1 + \Delta^{(1)} + \Delta^{(2)}\right), \quad (6)$$

where $\Delta^{(1)}$ ($\Delta^{(2)}$) denotes the $\mathcal{O}(\alpha_s)$ ($\mathcal{O}(\alpha_s^2)$) QCD corrections. Analytical results for $\Delta^{(2)}$ are presented for production near threshold [2] or by high energy expansions [4] with which we compare our numerical results.

Fig. 1 shows detailed comparison of our numerical results with the threshold [2] and high-energy expansion results [4] in a wide range of collision energies. It can be seen that our full results works well in the entire energy region, i.e., approaching the threshold results at lower energies and the high-energy expansions on the other end. The $\mathcal{O}(\alpha_s^2)$ correction can reach as large as 80% for $\sqrt{s} = 350\,\mathrm{GeV}$, due to threshold Coulomb singularities. On the other hand it is about 2% for intermediate collision energies and deacrease quickly to below 1% for high

[2] We count m_t and $\sqrt{s}$, the center-of-mass energy, the same order.

energies. The good agreements of our results on total cross sections with ones from threshold and high-energy expansions in the corresponding energy region furhther demonstrate the validity of our calculation.

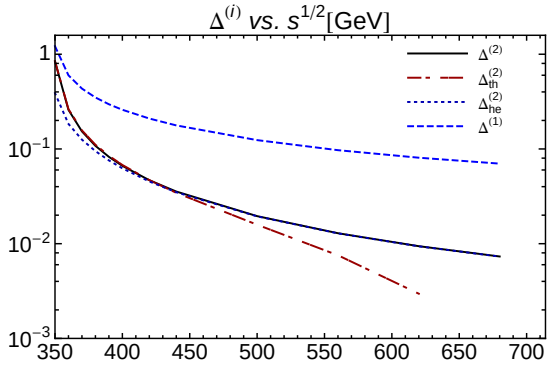

FIG. 1. Comparison of $\mathcal{O}(\alpha_s^2)$ corrections to total cross sections, $\Delta^{(2)}$, with the threshold results $\Delta_{th}^{(2)}$ and high-energy expansion results $\Delta_{he}^{(2)}$, as functions of collision energies.

Differential distributions and A_{FB}. We can calculate fully differential distributions up to NNLO in QCD based on the phase space slicing method. At LO, there is only one non-trivial kinematic variable, which we can choose either as cosine of the scattering angle between the final-state top quark and the initial-state electron $\cos\theta_t$, or transverse momentum of the top quark with respect to the beam line direction $p_{T,t}$. Similar to the inclusive cross section, we can define the $\mathcal{O}(\alpha_s)$ and $\mathcal{O}(\alpha_s^2)$ corrections for each kinematic bin, $\Delta_{bin}^{(1)}$ and $\Delta_{bin}^{(2)}$, in analogy to Eq. (6). The results are shown in Fig. 2 for $\cos\theta_t$ and Fig. 3 for $p_{T,t}$ distributions with a typical collision energies of 400 GeV. The $\mathcal{O}(\alpha_s^2)$ corrections are about one fourth of the $\mathcal{O}(\alpha_s)$ corrections for the total cross section. However, they show a different kinematic dependence. From Fig. 2 we can see both the $\mathcal{O}(\alpha_s)$ and $\mathcal{O}(\alpha_s^2)$ corrections are larger in forward direction and thus will increase the FB asymmetry. Moreover, the differences of $\Delta_{bin}^{(2)}$ in forward and backward region are of similar size as for $\Delta_{bin}^{(1)}$. Thus the $\mathcal{O}(\alpha_s^2)$ corrections to A_{FB} are as important as the $\mathcal{O}(\alpha_s)$ corrections as will be shown later. The transverse momentum distribution in Fig. 3 shows a different feature comparing to the angular distribution since they are also affected by the energy spectrum of the top quark. The real corrections pull the energy spectrum to the lower end and thus the $p_{T,t}$ distribution as well. As shown in Fig. 3, the $\mathcal{O}(\alpha_s^2)$ corrections start as positive in low p_T and then decrease to negative values near the kinematic limits. The $\mathcal{O}(\alpha_s^2)$ corrections show a relatively larger impact in the $p_{T,t}$ distribution.

The forward-backward asymmetry A_{FB} is defined as the number of top quark observed in the forward direction minus the one observed in the backward direction,

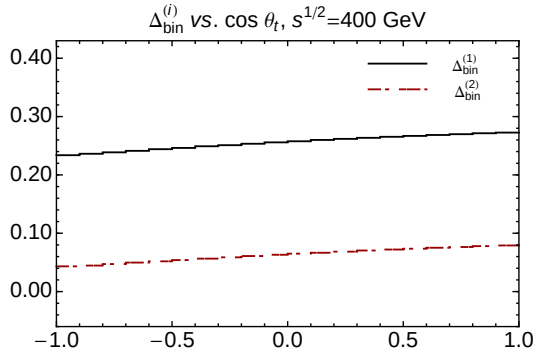

FIG. 2. $\mathcal{O}(\alpha_s)$ and $\mathcal{O}(\alpha_s^2)$ corrections in different $\cos\theta$ bins of top quark, $\Delta_{bin}^{(1)}$ and $\Delta_{bin}^{(2)}$, for $\sqrt{s} = 400$ GeV.

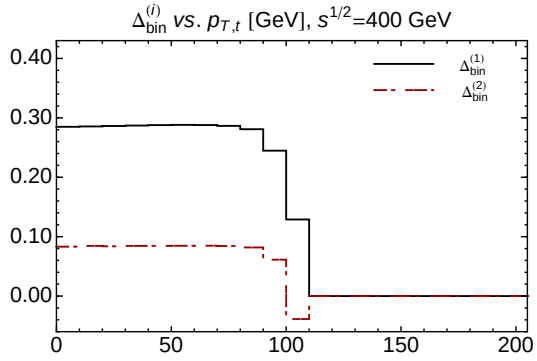

FIG. 3. $\mathcal{O}(\alpha_s)$ and $\mathcal{O}(\alpha_s^2)$ corrections in different p_T bins of top quark, $\Delta_{bin}^{(1)}$ and $\Delta_{bin}^{(2)}$, for $\sqrt{s} = 400$ GeV.

divided by the total number of top quark observed,

$$A_{FB} = \frac{\sigma_A}{\sigma_S} \equiv \frac{\sigma(\cos\theta_t > 0) - \sigma(\cos\theta_t < 0)}{\sigma(\cos\theta_t > 0) + \sigma(\cos\theta_t < 0)}, \qquad (7)$$

We show A_{FB} at LO as a function of the collision energy in the lower inset of Fig. 4. The A_{FB} at NLO and NNLO are calculated by using the corresponding NLO and NNLO cross sections in both the denominator and numerator of Eq. (7), and are shown in the upper inset of Fig. 4 normalized to the A_{FB} at LO. The $\mathcal{O}(\alpha_s)$ correction is about 2% for $\sqrt{s}$ around 500 GeV. The $\mathcal{O}(\alpha_s^2)$ correction further increases A_{FB} by about 1.2% in the same region. We also plot the A_{FB} calculated using the two-loop threshold cross sections [13] for comparison, which shows good agreement with our exact result in energy region just above the production threshold. This is expected since in the threshold region the former ones are dominant. We further investigate uncertainties of predictions on A_{FB} due to missing corrections beyond NNLO. A conventional way to estimate those uncertainties is by checking the residual QCD scale dependence. However, for ratios like A_{FB}, if we vary the scales simultaneously in σ_A and σ_S, it tends to be too optimistic. For example, the NLO prediction with scale uncertainty does not

$\sqrt{s}$ [GeV]	A_{FB}^{LO}	A_{FB}^{NLO}	A_{FB}^{NNLO}	δA_{FB}^{NNLO}
400	28.20	28.94 ± 0.76	29.58 ± 0.46	± 0.26
500	41.56	42.39 ± 0.59	42.89 ± 0.25	± 0.12
800	53.68	53.91 ± 0.33	54.07 ± 0.08	± 0.04

TABLE I. Top-quark forward-backward asymmetry at different perturbative orders for representative $\sqrt{s}$ values. All values are shown in percentage.

overlap with the NNLO prediction. Thus a more appropriate prescription is to vary the scales independently in σ_A and σ_S. We change the scale by a factor of two upward and downward in both σ_A and σ_S, and add the fractional uncertainties to A_{FB} in quadrature. The resulting uncertainties are shown in Fig. 4 by the colored bands. With the $\mathcal{O}(\alpha_s^2)$ corrections the scale uncertainty on A_{FB} has been reduced to less than half of the value at NLO as further shown in Table. I. The third and fourth columns of Table. I show the NLO and NNLO predictions of A_{FB} together with the scale uncertainties all shown in percentage. The column δA_{FB}^{NNLO} represents variation of FB asymmetry due to uncertainty of top-quark mass input, which is taken to be ± 0.5 GeV simply for comparison. For a typical collision energy of 500 GeV, the residual scale uncertainty of NNLO prediction on A_{FB} is 0.0025 or half percent in relative, which is well below the projected experimental precision of future ILC [16]. The uncertainty due to top quark mass input is relatively small especially considering the projected precision on mass measurement at the ILC.

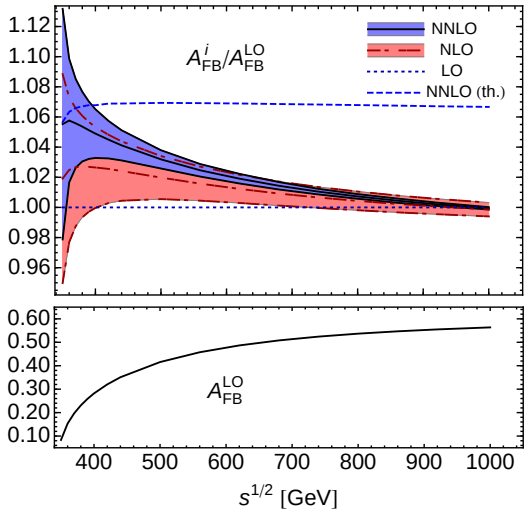

FIG. 4. Lower inset: top quark A_{FB} at the LO as a function of collision energy; upper inset: ratios of A_{FB} at the NLO and NNLO to A_{FB} at the LO. The threshold approximation is denoted as `th.`.

We can also look at top-quark FB asymmetry at a more exclusie level, namely the FB asymmetry in different $|\cos\theta_t|$ bins, $A_{FB,bin}$. In Fig. 5 we plot ratios of the NLO and NNLO predictions on $A_{FB,bin}$ to the LO ones for $\sqrt{s} = 400$ GeV. Both the $\mathcal{O}(\alpha_s)$ and $\mathcal{O}(\alpha_s^2)$ corrections are almost flat on $|\cos\theta_t|$ for $\sqrt{s} = 400$ GeV, but decrease slightly with $|\cos\theta_t|$ for $\sqrt{s} = 500$ GeV which is not shown here due to limited space.

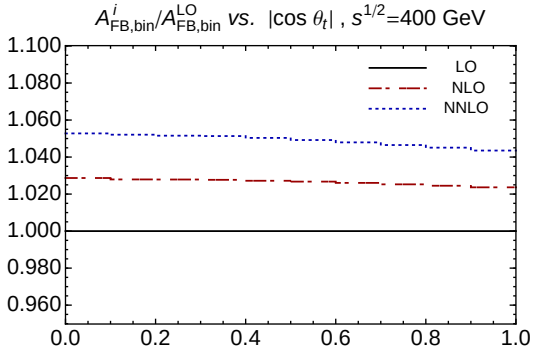

FIG. 5. Top-quark forward-backward asymmetry in different $|\cos\theta_t|$ bins, $A_{FB,bin}$, normalized to the LO predictions, for $\sqrt{s} = 400$ GeV.

Conclusions. We have presented the first complete NNLO QCD corrections to top-quark pair production at e^+e^- collisions. The calculation is at fully differential level based on a generalization of phase slicing method to NNLO in QCD [7]. Especially we study in detail the corrections to top-quark forward-backward asymmetry A_{FB}. The NNLO correction to A_{FB} is half of the size of the NLO corrections or even larger, for a typical collision energy of $400 \sim 500$ GeV at future linear colliders. Moreover, our results show a large reduction in the theoretical uncertainties on predictions of A_{FB}. The residual scale uncertainty is well below the projected experimental precision. Our results allow a precise determination of the top-quark neutral-current couplings at future linear colliders and thus the probe of various new physics beyond the SM. Besides, there could be several interesting applications of the method and results presented here. Firstly, it would be interesting to apply this calculation to charm and bottom quark production at Z boson mass pole. Secondly, decay of Higgs boson to massive quark can be calculated in the same way to NNLO in QCD, since the two-loop matrix elements are available [28]. Thirdly, it should be straightforward to combine production and leptonic decay [8, 29] of top-quark pair in e^+e^- collisions within narrow width approximation at NNLO. Last but not least, our calculation may also be used to improve the accuracy of event shape resummation related to heavy quark mass measurement [30].

This work was supported by the U.S. DOE under contract DE-AC02-76SF00515, Early Career Research Award DE-SC0003870 by Lightner-Sams Foundation, and Munich Institute for Astro- and Particle Physics (MIAPP) of the DFG cluster of excellence "Origin and

Structure of the Universe". Work at ANL is supported in part by the U.S. Department of Energy under Contract No. DE-AC02-06CH11357. HXZ thanks the theory group of Paul Scherrer Institute (PSI) at Zurich and the Center for Future High Energy Physics (CFHEP) at Beijing for hospitality where the project is finalized.

* jgao@anl.gov
† hxzhu@slac.stanford.edu

[1] H. Baer, T. Barklow, K. Fujii, Y. Gao, A. Hoang, S. Kanemura, J. List and H. E. Logan *et al.*, arXiv:1306.6352 [hep-ph].

[2] A. Czarnecki and K. Melnikov, Phys. Rev. Lett. **80**, 2531 (1998) [hep-ph/9712222]. M. Beneke, A. Signer and V. A. Smirnov, Phys. Rev. Lett. **80**, 2535 (1998) [hep-ph/9712302]. A. H. Hoang and T. Teubner, Phys. Rev. D **58**, 114023 (1998) [hep-ph/9801397]. M. Beneke, A. Signer and V. A. Smirnov, Phys. Lett. B **454**, 137 (1999) [hep-ph/9903260].

[3] M. Beneke, Y. Kiyo, P. Marquard, A. Penin, J. Piclum, D. Seidel and M. Steinhauser, Phys. Rev. Lett. **112**, 151801 (2014) [arXiv:1401.3005 [hep-ph]].

[4] S. G. Gorishnii, A. L. Kataev and S. A. Larin, Nuovo Cim. A **92**, 119 (1986). K. G. Chetyrkin and J. H. Kuhn, Phys. Lett. B **248**, 359 (1990). K. G. Chetyrkin and J. H. Kuhn, Nucl. Phys. B **432**, 337 (1994) [hep-ph/9406299]. R. Harlander and M. Steinhauser, Eur. Phys. J. C **2**, 151 (1998) [hep-ph/9710413]. K. G. Chetyrkin, R. Harlander, J. H. Kuhn and M. Steinhauser, Nucl. Phys. B **503**, 339 (1997) [hep-ph/9704222].

[5] W. Bernreuther, R. Bonciani, T. Gehrmann, R. Heinesch, T. Leineweber, P. Mastrolia and E. Remiddi, Nucl. Phys. B **706**, 245 (2005) [hep-ph/0406046]. W. Bernreuther, R. Bonciani, T. Gehrmann, R. Heinesch, T. Leineweber, P. Mastrolia and E. Remiddi, Nucl. Phys. B **712**, 229 (2005) [hep-ph/0412259]. W. Bernreuther, R. Bonciani, T. Gehrmann, R. Heinesch, T. Leineweber and E. Remiddi, Nucl. Phys. B **723**, 91 (2005) [hep-ph/0504190]. J. Gluza, A. Mitov, S. Moch and T. Riemann, JHEP **0907**, 001 (2009) [arXiv:0905.1137 [hep-ph]].

[6] W. Bernreuther, A. Brandenburg and P. Uwer, Phys. Rev. Lett. **79**, 189 (1997) [hep-ph/9703305]. G. Rodrigo, A. Santamaria and M. S. Bilenky, Phys. Rev. Lett. **79**, 193 (1997) [hep-ph/9703358]. P. Nason and C. Oleari, Phys. Lett. B **407**, 57 (1997) [hep-ph/9705295]. A. Brandenburg and P. Uwer, Nucl. Phys. B **515**, 279 (1998) [hep-ph/9708350]. P. Nason and C. Oleari, Nucl. Phys. B **521**, 237 (1998) [hep-ph/9709360]. G. Rodrigo, M. S. Bilenky and A. Santamaria, Nucl. Phys. B **554**, 257 (1999) [hep-ph/9905276].

[7] J. Gao and H. X. Zhu, arXiv:1408.5150 [hep-ph].

[8] J. Gao, C. S. Li and H. X. Zhu, Phys. Rev. Lett. **110**, 042001 (2013) [arXiv:1210.2808 [hep-ph]].

[9] A. von Manteuffel, R. M. Schabinger and H. X. Zhu, arXiv:1408.5134 [hep-ph].

[10] A. Gehrmann-De Ridder, T. Gehrmann and E. W. N. Glover, JHEP **0509**, 056 (2005) [hep-ph/0505111]. W. Bernreuther, C. Bogner and O. Dekkers, JHEP **1106**, 032 (2011) [arXiv:1105.0530 [hep-ph]]. G. Abelof and A. Gehrmann-De Ridder, JHEP **1211**, 074 (2012) [arXiv:1207.6546 [hep-ph]]. G. Abelof, O. Dekkers and A. Gehrmann-De Ridder, JHEP **1212**, 107 (2012) [arXiv:1210.5059 [hep-ph]]. W. Bernreuther, C. Bogner and O. Dekkers, JHEP **1310**, 161 (2013) [arXiv:1309.6887 [hep-ph]]. G. Abelof, A. Gehrmann-De Ridder, P. Maierhofer and S. Pozzorini, arXiv:1404.6493 [hep-ph]. G. Abelof and A. G. D. Ridder, arXiv:1409.3148 [hep-ph].

[11] O. Dekkers and W. Bernreuther, arXiv:1409.3124 [hep-ph].

[12] G. Altarelli and B. Lampe, Nucl. Phys. B **391**, 3 (1993). V. Ravindran and W. L. van Neerven, Phys. Lett. B **445**, 214 (1998) [hep-ph/9809411]. S. Catani and M. H. Seymour, JHEP **9907**, 023 (1999) [hep-ph/9905424].

[13] W. Bernreuther, R. Bonciani, T. Gehrmann, R. Heinesch, T. Leineweber, P. Mastrolia and E. Remiddi, Nucl. Phys. B **750**, 83 (2006) [hep-ph/0604031].

[14] K. Agashe, R. Contino and R. Sundrum, Phys. Rev. Lett. **95**, 171804 (2005) [hep-ph/0502222]; M. S. Carena, E. Ponton, J. Santiago and C. E. M. Wagner, Nucl. Phys. B **759**, 202 (2006) [hep-ph/0607106]; R. Contino, T. Kramer, M. Son and R. Sundrum, JHEP **0705**, 074 (2007) [hep-ph/0612180].

[15] R. S. Chivukula, S. B. Selipsky and E. H. Simmons, Phys. Rev. Lett. **69**, 575 (1992) [hep-ph/9204214]; R. S. Chivukula, E. H. Simmons and J. Terning, Phys. Lett. B **331**, 383 (1994) [hep-ph/9404209]; A. Pomarol and J. Serra, Phys. Rev. D **78**, 074026 (2008) [arXiv:0806.3247 [hep-ph]];

[16] E. Devetak, A. Nomerotski and M. Peskin, Phys. Rev. D **84**, 034029 (2011) [arXiv:1005.1756 [hep-ex]].

[17] M. S. Amjad, M. Boronat, T. Frisson, I. Garcia, R. Poschl, E. Ros, F. Richard and J. Rouene *et al.*, arXiv:1307.8102.

[18] M. S. Amjad, T. Frisson, E. Kou, R. Poschl, F. Richard and J. Rouene, Nuovo Cim. C **037**, no. 02, 55 (2014).

[19] S. Frixione, Z. Kunszt and A. Signer, Nucl. Phys. B **467**, 399 (1996) [hep-ph/9512328].

[20] S. Catani and M. H. Seymour, Nucl. Phys. B **485**, 291 (1997) [Erratum-ibid. B **510**, 503 (1998)] [hep-ph/9605323].

[21] G. Cullen, H. van Deurzen, N. Greiner, G. Heinrich, G. Luisoni, P. Mastrolia, E. Mirabella and G. Ossola *et al.*, arXiv:1404.7096 [hep-ph].

[22] P. Mastrolia, E. Mirabella and T. Peraro, JHEP **1206**, 095 (2012) [Erratum-ibid. **1211**, 128 (2012)] [arXiv:1203.0291 [hep-ph]].

[23] T. Peraro, Comput. Phys. Commun. **185**, 2771 (2014) [arXiv:1403.1229 [hep-ph]].

[24] A. van Hameren, C. G. Papadopoulos and R. Pittau, JHEP **0909**, 106 (2009) [arXiv:0903.4665 [hep-ph]].

[25] A. van Hameren, Comput. Phys. Commun. **182**, 2427 (2011) [arXiv:1007.4716 [hep-ph]].

[26] A. Denner and T. Sack, Nucl. Phys. B **358**, 46 (1991).

[27] J. Beringer *et al.* [Particle Data Group Collaboration], Phys. Rev. D **86**, 010001 (2012).

[28] W. Bernreuther, R. Bonciani, T. Gehrmann, R. Heinesch, P. Mastrolia and E. Remiddi, Phys. Rev. D **72**, 096002 (2005) [hep-ph/0508254].

[29] M. Brucherseifer, F. Caola and K. Melnikov, JHEP **1304**, 059 (2013) [arXiv:1301.7133 [hep-ph]].

[30] S. Fleming, A. H. Hoang, S. Mantry and I. W. Stewart,
Phys. Rev. D **77**, 074010 (2008) [hep-ph/0703207].